Furnace for *in situ* and simultaneous studies of nano-precipitates and phase transformations in steels by SANS and neutron diffraction

A. Navarro-López, C. Ioannidou, E. M. van der Wal, Z. Arechabaleta, R. van den Oever, M. N. Verleg, R. M. Dalgliesh, J. Sykora, F. A. Akeroyd, N. Geerlofs, J. Sietsma, C. Pappas, A. A. van Well, and S. E. Offerman

View Online   **Export Citation**   **CrossMark**

ARTICLES YOU MAY BE INTERESTED IN

Furnace for *in situ* and simultaneous studies of nano-precipitates and phase transformations in steels by SANS and neutron diffraction

A. Navarro-López,[1,a] C. Ioannidou,[1] E. M. van der Wal,[2] Z. Arechabaleta,[1,b] R. van den Oever,[2] M. N. Verleg,[2] R. M. Dalgliesh,[3] J. Sykora,[3] F. A. Akeroyd,[3] N. Geerlofs,[1] J. Sietsma,[1] C. Pappas,[2] A. A. van Well,[2] and S. E. Offerman[1]

AFFILIATIONS

[1] Department of Materials Science and Engineering, Delft University of Technology, Mekelweg 2, 2628 CD Delft, The Netherlands
[2] Department of Radiation Science and Technology, Delft University of Technology, Mekelweg 15, 2629 JB Delft, The Netherlands
[3] ISIS Neutron and Muon Source, Rutherford Appleton Laboratory, Oxfordshire OX11 0QX, United Kingdom

[a] Author to whom correspondence should be addressed: a.navarrolopez@tudelft.nl
[b] Present address: Tecnalia Research & Innovation, Geldo, Derio, Spain.

ABSTRACT

Interphase precipitation occurring during solid-state phase transformations in micro-alloyed steels is generally studied through transmission electron microscopy, atom probe tomography, and *ex situ* measurements of Small-Angle Neutron Scattering (SANS). The advantage of SANS over the other two characterization techniques is that SANS allows for the quantitative determination of size distribution, volume fraction, and number density of a statistically significant number of precipitates within the resulting matrix at room temperature. However, the performance of *ex situ* SANS measurements alone does not provide information regarding the probable correlation between interphase precipitation and phase transformations. This limitation makes it necessary to perform *in situ* and simultaneous studies on precipitation and phase transformations in order to gain an in-depth understanding of the nucleation and growth of precipitates in relation to the evolution of austenite decomposition at high temperatures. A furnace is, thus, designed and developed for such *in situ* studies in which SANS measurements can be simultaneously performed with neutron diffraction measurements during the application of high-temperature thermal treatments. The furnace is capable of carrying out thermal treatments involving fast heating and cooling as well as high operation temperatures (up to 1200 °C) for a long period of time with accurate temperature control in a protective atmosphere and in a magnetic field of up to 1.5 T. The characteristics of this furnace give the possibility of developing new research studies for better insight of the relationship between phase transformations and precipitation kinetics in steels and also in other types of materials containing nano-scale microstructural features.

I. INTRODUCTION

Precipitation in steels has been extensively studied over the years since the formation of precipitates within the steel microstructure often entails an enhancement of its mechanical behavior. The improvement of steel strength due to precipitation can occur via different mechanisms in which precipitates reduce the mobility of dislocations, inhibit grain growth, or even suppress recrystallization via the pinning of dislocations and grain boundaries.[1,2]

In micro-alloyed steels, the process of formation and growth of precipitates can typically take place in different phases: (I) precipitation in the fcc phase (austenite),[3] (II) precipitation in bcc phases (generally, ferrite or martensite),[4–6] and (III) precipitation during fcc-to-bcc transformation (mainly austenite-to-ferrite).[7–10] The last one is commonly known as interphase precipitation.

The complex processes of nucleation and growth of precipitates of different sizes and morphologies inherent to each type of precipitation make it necessary to use several advanced

characterization techniques for a better understanding of the underlying precipitation mechanisms. Among all the possible techniques to be used, Small-Angle Neutron Scattering (SANS) is one of the most powerful characterization techniques extensively used to study the precipitation phenomenon in a wide range of steel compositions.[3,4,6,8–13] This non-destructive technique provides statistically relevant and quantitative information concerning the size distribution, volume fraction, and number density of precipitates. The SANS measurements can be performed *in situ* at a specific temperature range where precipitation takes place or *ex situ* at room temperature after the application of a thermal treatment. For ferromagnetic materials, a strong magnetic field may need to be applied in both types of SANS measurements to avoid any contribution from magnetic-domain scattering.

Precipitation in austenite has been studied by *in situ* SANS measurements at high temperature ranges where austenite is present in the steel microstructure,[3] without the need for a strong magnetic field since austenite is in the paramagnetic state. On the other hand, precipitation in ferritic (or martensitic) steels is mainly studied by *ex situ* SANS measurements after the application of annealing (or aging) treatments at intermediate temperatures (below the A_1 temperature).[4,6] These measurements require a large magnetic field to avoid the magnetic-domain scattering from ferromagnetic phases, such as ferrite (or martensite). However, both the current *in situ* and *ex situ* SANS measurements present certain limitations: (1) the need for the combination of a furnace and an electromagnet to perform *in situ* SANS measurements of precipitation in ferro-magnetic materials and (2) the interference in *ex situ* measurements of the SANS-signal from precipitates with the SANS-signal from other microstructural features, such as the dislocations contained in a martensitic microstructure, respectively.

Interphase precipitation during austenite-to-ferrite phase transformation is generally studied by *ex situ* SANS measurements performed at room temperature and in a magnetic field to prevent magnetic-domain scattering.[8–10] The progress of the formation and growth of precipitates during the austenite-to-ferrite phase transformation is, thus, studied from a series of partially transformed (and partially precipitated) microstructures after being annealed for several holding times followed by subsequent rapid cooling to room temperature. This implies the formation of a certain volume fraction of ferrite, depending on the holding time, as well as the formation of other phases, generally martensite, during the final cooling. The limitations of these *ex situ* SANS measurements are (1) the overlapping of the SANS-signals from the precipitates and from other microstructural features, generally from the high density of dislocations formed in martensite, and (2) the difficulty in obtaining an accurate background from a reference microstructure free of precipitates and other microstructural features contributing to the SANS-signal.

Due to the limitations of *ex situ* SANS measurements, precipitation occurring during austenite-to-ferrite phase transformation in steels may be studied more accurately by *in situ* SANS measurements during the application of thermal treatments at relatively high temperatures where both phenomena take place. This implies that the use of a furnace as well as an electromagnet is, thus, essential to perform such *in situ* measurements and overcome the corresponding limitations. Furthermore, an additional simultaneous

characterization technique can be used with SANS to track the progress of the phase transformation and be able to relate it with the formation and growth of precipitates within the microstructure. Neutron diffraction (ND) is the most appropriate characterization technique to be used for such studies since it is also a non-destructive technique capable of providing quantitative information regarding the evolution of volume fraction of phases during any phase transformation.

Several furnaces were developed with the objective of performing experimental measurements through SANS, high-energy x-ray diffraction (HE-XRD), or ND for the *in situ* study of precipitation, phase transformations, and/or mechanical performance at high temperatures in different types of metals.[14–22] Most of these furnaces were able to operate at temperatures up to 1300 °C under a protective atmosphere by either vacuum or an inert gas. However, none of the referenced furnaces were designed for *in situ* and simultaneous studies of both phenomena by the use of two of the characterization techniques previously mentioned (SANS, HE-XRD, and ND). In the case of steels, the need for applying a magnetic field when studying precipitation in a ferro-magnetic material by using neutrons entails a limiting design criterion, since the furnace should fit between the poles of an electromagnet, which is not the case for the referenced furnaces.

In a research study of the formation of precipitates and dislocations in a micro-alloyed steel, *in situ* diffraction and small-angle scattering measurements were carried out in a multi-purpose furnace using x-rays.[5,23] Although high-energy x-ray radiation is used in such studies, the contrast given by x-rays between the precipitates and the matrix may be insufficient for an accurate precipitation analysis in the case of similar electron densities between the matrix and the precipitate. An alternative to solve this limitation is the use of neutrons since they are more suitable than x-rays for studying precipitation in cases where the electron density difference between the precipitate and the matrix is small. Neutrons can give a larger contrast than x-rays between the precipitates and the matrix, resulting in higher quality measurements, because neutron scattering length densities may be significantly different between the precipitate and the matrix. In addition, the use of neutrons in *in situ* measurements also allows the determination of the evolution of the chemical composition of the precipitates with the progress of the phase transformation through the analysis of the nuclear and magnetic contributions of the neutrons scattering signal.[24]

The combination of SANS and ND for *in situ* measurements during the application of thermal treatments is, thus, the most promising alternative for further in-depth research on interphase precipitation in micro-alloyed steels. Within Europe, the Larmor Instrument placed at ISIS STFC Rutherford Appleton Laboratory (UK) is the only facility in which both techniques can simultaneously be used for such studies. In the near future, the European Spallation Source (ESS) will also give the opportunity of carrying out this type of research studies with the combined use of both techniques.[25] With this aim, the development of a furnace suitable for the simultaneous study with neutrons of precipitation and phase transformations in steels is needed and, in turn, is expected to contribute to better insight of both phenomena. The furnace will also be suitable for the study of any material with nano-scale microstructural features in a magnetic or non-magnetic matrix. This

research work describes the general design requirements as well as the main components of a furnace specially designed and developed to perform *in situ* and simultaneous SANS and ND measurements. The design of the control system needed to use the furnace successfully is also described. Furthermore, a basic analysis of the first *in situ* SANS measurements in combination with ND measurements during the application of thermal treatments with the designed furnace is presented to establish the performance of the furnace and show a new research alternative to study the relationship between phase transformation and precipitation kinetics.

II. DESIGN REQUIREMENTS

The design requirements for a furnace to be developed for simultaneous studies of interphase precipitation and phase transformations in micro-alloyed steels are defined not only by the thermal treatments necessary to apply for such studies, but also by the spatial and geometrical limitations imposed by the Larmor Instrument at ISIS STFC Rutherford Appleton Laboratory (UK), which is used for the SANS and ND measurements in combination with an electromagnet. Table I shows a summary of the main requirements for the furnace design.

TABLE I. General requirements for the furnace design.

Furnace height	Maximum height of 44 mm, which is the maximum distance between the available electromagnet poles to reach magnetic saturation (1.5 T) of steel specimens at elevated temperatures
Material of the furnace	Non-magnetic material Machinable Minimum yield strength 100 MPa to resist the pressure difference between vacuum in the furnace and ambient pressure
Windows	Vacuum tight Resist the pressure difference between vacuum in the furnace and ambient pressure Non-magnetic material Neutron transparent Same thermal expansion coefficient with the furnace material Size and position depends on the beam size and position of the SANS and ND detectors
Heat shields	Non-magnetic material Resist a minimum temperature of 1200 °C High heat reflection coefficient (reflectance)
Temperature control	High temperature (up to 1200 °C) to dissolve all carbides/carbonitrides Accurate control (± 1 °C) Temperature gradient in the irradiated volume less than 0.3 °C/mm Heating rate (~10 °C/s), but not critical Necessary to reach cooling rates higher than 15 °C/s to avoid phase transformation and precipitation before annealing
Atmosphere control	Minimum vacuum of the order of 10^{-4} mbar (avoiding oxidation and decarburization of steel specimens) Gas for specimen cooling (He)
Specimen	I-shaped (approx. Gauge dimensions $10 \times 14 \times 1$ mm^3)
Specimen holder	Allow sample thermal expansion without deformation
Specimen change	Fast and easy
Specimen rotation	Maximum rotation angle of 20° Accurate and user-friendly control system Compact equipment due to the reduced room available for the setup

One of the main criteria for the furnace design is related to the spatial and geometrical requirements. The use of a steel specimen requires, for SANS data collection, that it is magnetically saturated during the application of any thermal treatment to prevent small-angle scattering from magnetic domains. The magnetic field (1.5 T) needed to reach magnetic saturation is directly related to the gap between the 75 mm diameter pole shoes of a GMW-3473 dipole electromagnet.[26] This gap is limited to a maximum of 44 mm for the previously mentioned magnetic field. The GMW electromagnet is placed in a vertical configuration with the furnace between its pole shoes, as shown in Fig. 1(a). The longest dimension of the specimen should be parallel to the magnetic field since, in this case, the demagnetization factor is the smallest.

Another important design criterion is related to the definition of the thermal treatment with an accurate control of the time–temperature profile to obtain the desired final microstructure. The furnace should be able to heat the steel specimen at moderate rates (between $1\,°C/s$ and $20\,°C/s$) up to a maximum temperature of $1200\,°C$, at which the specimen can be held for a certain time (up to 15 min–20 min) to assure that carbon and all other alloying elements are in solid solution. During cooling, the maximum rate should be rapid enough (up to $20\,°C/s$) to ensure the application of thermal treatments without any phase transformation during continuous cooling. After the interrupted cooling, isothermal holdings

FIG. 1. (a) Initial design of the general experimental setup and (b) schematic top view (not on scale) of the experimental setup with the position of main elements. The shown specimen orientation corresponds with the 0° position of the steel specimen with respect to the incoming neutron beam.

in a wide range of temperatures should be possible to be applied for long periods of time (up to 10 h), maintaining the capability and feasibility of the furnace.

Both criteria are the basis of the furnace design since the material used to build the furnace should be, on one hand, a machinable non-magnetic material and, on the other hand, a material with high resistance to high temperatures and good thermal conductivity. Apart from these requirements, the windows of the furnace, i.e., the furnace areas interfering with the incoming and scattered neutron beams, should be as thin as possible to minimize the interaction with the neutron beams. In addition, the furnace windows must be made of a material that is not significantly activated by the neutron beam and has minimum absorption of the neutron signal (<10%). For SANS measurements, the material of the furnace windows should give a small background signal compared to that given by the specimen. The background signal should also be constant to ensure that no microstructural changes occur in the window material during the application of thermal treatments. For ND measurements, the main requirement lies in preventing the overlap, insofar as possible, of the diffraction peaks corresponding to the windows' material with the ones obtained from the specimen.

The third design criterion to be considered is related to the temperature distribution along the specimen since high temperature gradients could cause local differences in phase transformation and precipitation starting at different specimen areas. The thermal gradient along the area probed by the incident neutron beam should be as small as possible to ensure that the temperature measured with a spot-welded thermocouple close to that area is the same as the temperature defined in the programmed thermal treatment. Reaching and maintaining a high temperature of the specimen require the introduction of heat shields within the furnace chamber, which are made of a non-magnetic, high-temperature resistant, and heat-reflective material. Moreover, the furnace should be able to endure the pressure difference between the ambient pressure and the vacuum level within the furnace chamber during the heating and holding stages as well as the expansive effect caused by the introduction of pressurized gas during cooling. An appropriate level of vacuum within the furnace chamber is necessary to prevent decarburization and oxidation of the steel specimen during the application of the thermal treatment, but also neutron scattering from air. The furnace design should also allow fast and easy insertion/extraction of the specimen as well as its possible thermal expansion without deformation during the application of the thermal treatment.

Rotating the specimen around its vertical axis is the last main design criterion. Specimen rotation is needed in order to bring more grains in the diffraction condition when determining the mass fractions of ferrite and austenite. In this way, the effects of possible specimen texture induced by the pre-application of processes such as hot rolling are minimized. Ideally, the specimen should be rotated over 360° during the *in situ* measurements to minimize texture effects in the resulting neutron diffraction patterns, although smaller rotations are also possible.[27] This would imply the use of a cylindrical specimen. However, flat specimens are better suited for SANS measurements and, in this geometry, the rotation of the specimen is limited because the illuminated volume by the incident neutron beam varies with rotation. This limitation affects both the SANS and the ND measurements, becoming a challenge to the post-processing of
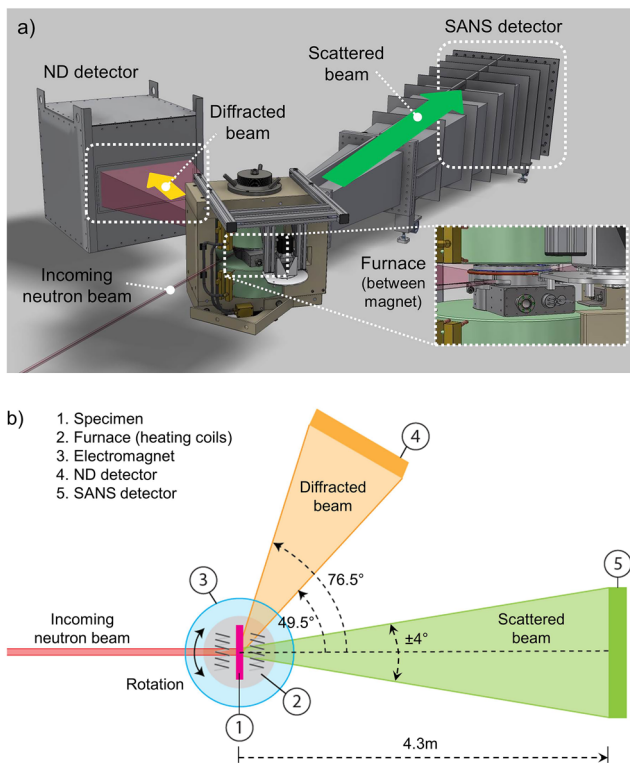
the generated experimental data. As a compromise, the specimen should be rotated over 20° during the application of the thermal treatment.

The possibility of rotating solely the specimen holder inside the furnace is discarded due to the limited space of the furnace chamber. The rotation of the whole furnace is, thus, the only option, although rotation is limited by the electromagnet. To facilitate the rotating movement of the furnace, placed between the pole shoes of the electromagnet, the furnace geometry should be cylindrical. A schematic top view of the experimental setup is depicted in Fig. 1(b), showing the 0° position of the specimen (perpendicular to the incident neutron beam) and the position of the SANS and ND detectors. For SANS measurements, the extension of the furnace windows is defined by the angular range covered by the SANS detector, limited to ±4°, and the rotation angle selected to reduce texture effects. For ND measurements, the specimen material determines the neutron diffraction angle and, as a result, the position of the furnace windows. Calculations of the diffraction angles for ferritic and austenitic steel specimens indicated that, for a wavelength range of 0.10 nm–0.35 nm, a 45°–80° angle range with respect to the incoming neutron beam is sufficient for detecting the first four diffraction peaks of each of the fcc- and bcc-phases. Thus, furnace windows are also defined by this angle range and the rotation angle selected to reduce texture effects in diffraction measurements.

III. FURNACE DESIGN

The final furnace design consists of the following components: (A) the outer furnace (lids and central section) including windows, (B) a heating cell, and (C) several heat shields. Depending on the requirements to fulfill, distinct materials are chosen to make each component. The material selection made for each of these components is described below. Moreover, a brief description is included on how (E), (F) the temperature and the protective atmosphere are controlled during the application of thermal treatments as well as (G) the specimen rotation.

A. Outer furnace (lids and central section) and windows

The material used for the upper/bottom lids as well as the central section of the furnace is the Al–Mg–Si1 aluminum alloy. This material is chosen because it is paramagnetic, thus non-(ferro)magnetic. It is easily machinable, so that the central section including the windows can be made out of one piece with reasonable strength. The selected material also provides a reasonably good compromise between strength and stiffness, which is crucial to maintain all parts of the outer furnace unaltered in shape, supporting the pressure difference when vacuum is made within the furnace chamber. In addition, this material is characterized by good thermal conductivity, which limits the deformation of the outer furnace throughout the fast heat dissipation during the thermal treatments.

The same aluminum Al–Mg–Si1 alloy is also selected for the furnace windows. The use of the same material eliminates the need for welding or clamping the windows to the central section. Although the selected material is transparent, to some extent, to neutrons, the windows are chosen to be 1 mm thick to minimize

their interference with the incoming and scattered neutron beams without compromising the robustness of the entire furnace. Note that, for this alloy, precipitation hardening can occur due to aging at temperatures higher than 80 °C–90 °C. The temperature of the furnace windows during the application of thermal treatments should, thus, be kept below this temperature in order to avoid the formation of precipitates in the aluminum windows, which could interfere with the SANS measurements. Last but not least, the diffraction peaks from these Al-windows do not interfere with the diffraction peaks of the steel for the experimental conditions used at Larmor Instrument.

B. Heating cell

The heating cell is placed in the center of the furnace and consists of a titanium frame, four molybdenum heat shields, and four boron-nitride cylinders with their respective molybdenum–lanthanum windings. The titanium frame does not interfere with the incident neutron beam. Two molybdenum heat shields are inserted at both sides in the titanium frame close to the specimen to reduce the heat loss as well as the thermal gradient along the specimen gauge. Two heating coils are placed at both specimen sides at the upper and bottom parts of the frame. A molybdenum–lanthanum wire of 0.5 mm diameter is selected for windings of the heating coil. This type of wire resists temperatures up to 2000 °C and exhibits better electrical behavior compared to other materials such as platinum, platinum-10%rhodium, or even molybdenum. The molybdenum–lanthanum wire is wound around a boron-nitride cylinder to give the coil good mechanical and thermal stability. Four heating coils are used to heat the specimen during the application of the thermal treatment. The titanium frame and the configuration of the heating system are shown in Figs. 2(a) and 2(b).

C. Outer heat shields

Several heat shields are concentrically placed between the heating cell and the outer furnace in order to reduce the heat loss and keep the temperature of the outer furnace as low as possible for safety reasons, and also to avoid possible precipitation hardening in the Al-windows. Molybdenum is selected as the optimum material for heat shields since it is easily machinable, resists high temperatures, and is not activated by neutron irradiation. The use of molybdenum heat shields allows higher temperatures to be reached in the steel specimen during heating than those reached when no heat shields are used, using the same power. Considering the room available between the heating cell and the outer furnace, seven heat shields of 0.15 mm thickness are placed within the furnace chamber. All heat shields have rectangular windows, as shown in Fig. 2(c), at locations that coincide with the angular openings for the incoming and scattered neutron beams indicated in Sec. II.

D. Specimen

I-shaped specimens with total dimensions of 32 mm height, 30 mm width, and 1 mm thickness are used for *in situ* and simultaneous SANS–ND measurements [see Fig. 2(d)]. The dimensions of the gauge area are 10 mm high and 14 mm wide. This specimen shape minimizes the heat thermal gradient in the gauge area. The stability of the specimen inside the titanium frame of the heating cell
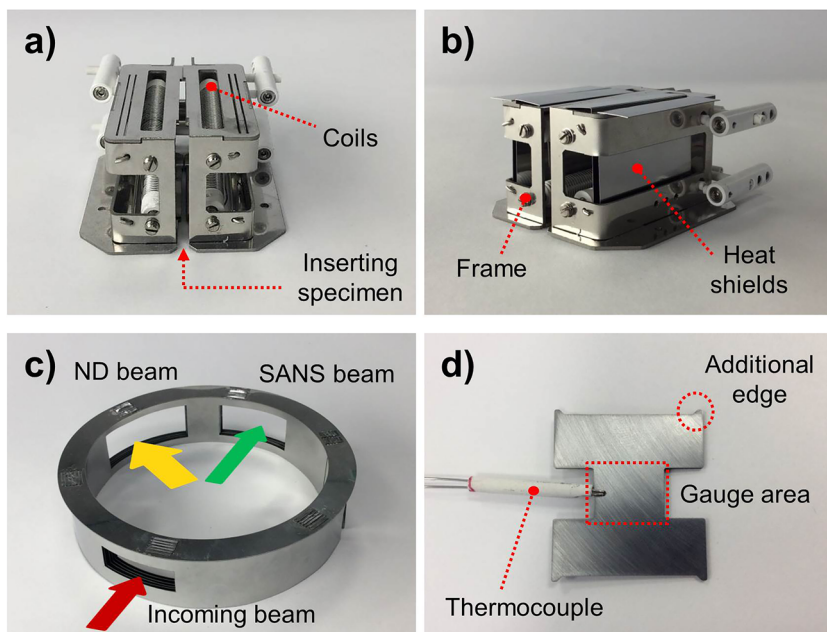
FIG. 2. (a) Heating cell containing the four boron-nitride cylinders with heating coils (windings) without the direct shielding system and (b) heating cell with two heat shields at both sides of the cell. The replacement of specimens is performed through the opposite side to the one in which all connections are placed. (c) Concentric molybdenum heat shields placed within the furnace chamber surrounding the heating cell. There are open windows to allow the neutron incident beam as well as the scattered and diffracted beams to pass through without interference. (d) Steel specimen used in the *in situ* experiments.

is achieved by the use of horizontal reels in the upper and bottom parts of the frame. The specimen has four additional edges to maintain its horizontal position within the frame and reduce the thermal conduction to the surroundings.

Figures 3(a)–3(d) show the different components of the furnace, such as the heating cell, the heat shielding system, the furnace chamber as well as a general overview of the final design of the multi-purpose furnace and the setup of all parts. As observed in Fig. 3(a), the heating cell is fixed within the furnace chamber in a position at which the incident neutron beam is perpendicular to the steel specimen. Figure 3(b) shows the final position of the concentrically disposed molybdenum heat shields as well as the central section of the furnace chamber. This section shows a gap in its center corresponding to the window of the incident neutron beam. Once the specimen is inserted in the heating cell, two replaceable molybdenum discs are placed at the top of the furnace chamber as additional
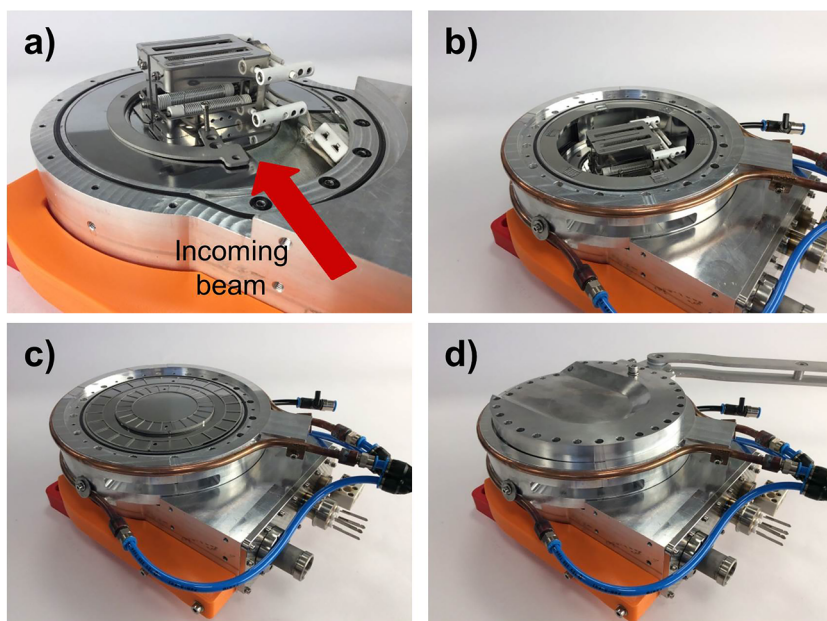

FIG. 3. Final design and setup of the heating cell, shielding system, and other additional parts of the furnace with 200 mm diameter and 44 mm height. (a) Placement and fixation system of the heating cell, (b) heating cell and shielding system within the furnace chamber, (c) additional molybdenum shielding on top of the heating cell, and (d) placement of the furnace lid with the rotation system.

heat shields [see Fig. 3(c)]. Figure 3(d) shows the final assembling of all parts of the furnace as well as a water cooling system consisted of two tubes wrapped around the upper and bottom part of the central section in order to cool down the furnace during the application of thermal treatments.

E. Temperature control

The specimen temperature at any time during the application of the thermal treatment is measured by two K-type thermocouples made of chromel–alumel wires of 0.5 mm each. Both thermocouples are spot-welded to the specimen. The main thermocouple, which is used for the temperature control, is placed at the side of the center of the specimen gauge. The second thermocouple, which gives insight of the possible temperature gradient, is placed in the center at the edge of the specimen gauge. Both thermocouple wires are isolated by an initial alumina tube followed by a fiberglass cover. After having determined a thermal gradient of $\Delta T \leq 0.3\,^{\circ}C/mm$ along the specimen gauge, one thermocouple is only used for the temperature control, as shown in Fig. 2(d), simplifying the experimental setup.

F. Atmospheric control

An inert atmosphere is created during the heating and holding stages of the thermal treatment by creating a vacuum inside the furnace chamber using a rotary pump. The airtight sealing is achieved by placing a rubber O-ring between the central section and the upper/bottom taps of the furnace [see Fig. 3(a)], which allows us to reach a vacuum level of the order of 10^{-4} mbar within the furnace chamber. The air within the chamber is extracted before the beginning of each *in situ* measurement, avoiding the oxidation and decarburization of the specimen at high temperatures as well as minimizing the heat transfer between the heating elements and the furnace frame that prevents an undesired warming up. During cooling, an inert atmosphere is created by flushing an inert gas, such as helium, through a gas system controlled by a mass-flow controller.

G. Specimen rotation

The optimum range of the specimen rotation angle is established between 0° and $+20^{\circ}$ (counter-clockwise direction), taking into consideration all the limitations derived from the use of an electromagnet and the specimen geometry. The asymmetric rotation of the furnace during *in situ* measurements reduces the possible attenuation of the diffracted neutron beam from the specimen with a flat geometry (needed for SANS), since the neutron diffraction detector is positioned laterally with respect to the direction of the incident neutron beam. The 0° position corresponds with that in which the specimen gauge area is perpendicular to the incident neutron beam, as depicted in Fig. 1(b). The rotation is performed by a stepper motor ($0.025^{\circ}/step$) connected with an arm to the furnace. Figure 3(d) shows this connection system where the arm of the rotation system is attached to one side of the upper lid of the furnace. The rotating movement consists of a forward–backward rotation over the specimen longitudinal axis within the selected rotation angle range. Although this rotation range does not allow the measurement of the full texture of the specimen, the volume fraction of fcc and bcc

phases can still be determined from the diffraction peaks assuming there is no change in texture during phase transformations.

IV. CONTROL SYSTEM DESIGN

The design characteristics of the furnace as well as the several requirements (heating, cooling, and rotation) needed to successfully achieve the desired results are considered in order to develop the final experimental setup for the performance of *in situ* SANS and ND measurements. As a brief summary, the equipment included in the final experimental setup is the following:

- Furnace (with all components described above).
- Temperature controller (Eurotherm 3504).
- Power supply (to provide power to the heating coils).
- Rotary pump (to make vacuum).
- Mass-flow controller (to cool down samples by helium gas).
- Stepper motor (including the rotation system).
- Local laptop (to control the entire setup).
- CompactRIO (interfacing with ISIS control systems,[28] data acquisition, and stepper motor control).

All mentioned equipment must be interconnected and, in turn, connected with the instrument control system of the ISIS Neutron Research Center in order to correctly perform the desired thermal treatments and exchange the resulting data, respectively. The general data acquisition and control system setup including all the connections is shown in Fig. 4. The components of the local control system are highlighted in blue color. A network time protocol (NTP) is used to ensure that the time reference of both systems is the same. This is crucial since the experimental data forwarded to the ISIS system are time-stamped. The start of each *in situ* SANS–ND measurement is defined by a hardware trigger signal, which is generated by the Larmor instrument control system. On the other hand, the start of the programmed thermal treatment, asynchronous to the Larmor instrument, is initiated by a manual action via the user interface of the local control system.

The Eurotherm controller is programmed with a predefined thermal profile that can be parameterized by the user. The control topology in the Eurotherm is implemented as a cascade proportional-integral-derivative (PID) control topology and is fine tuned to the system characteristics of the used peripheral system components. According to the programmed thermal treatment, the Eurotherm component controls the power supplied to the molybdenum–lanthanum windings for heating the specimen and the flow of helium gas necessary to flush into the furnace chamber for cooling the specimen. The maximum power given by the power supply is limited to 400 W (40 V–10 A). The pressure inside the furnace chamber is controlled by a pressure sensor and a valve. Furthermore, the Eurotherm controller receives as input signals the temperatures measured by three thermocouples placed in the specimen gauge center (TC1), at the edge of the specimen gauge (TC2), and at the upper lid of the furnace (TC3). All signals are also sent to the CompactRIO (cRIO) controller, which acts as the primary data interface to the in-place ISIS control system. For safety reasons, the CompactRIO controller switches off the power supply as soon as the temperature of the upper lid of the furnace, measured by the K-type thermocouple (TC3), exceeds the temperature of $100\,^{\circ}C$.
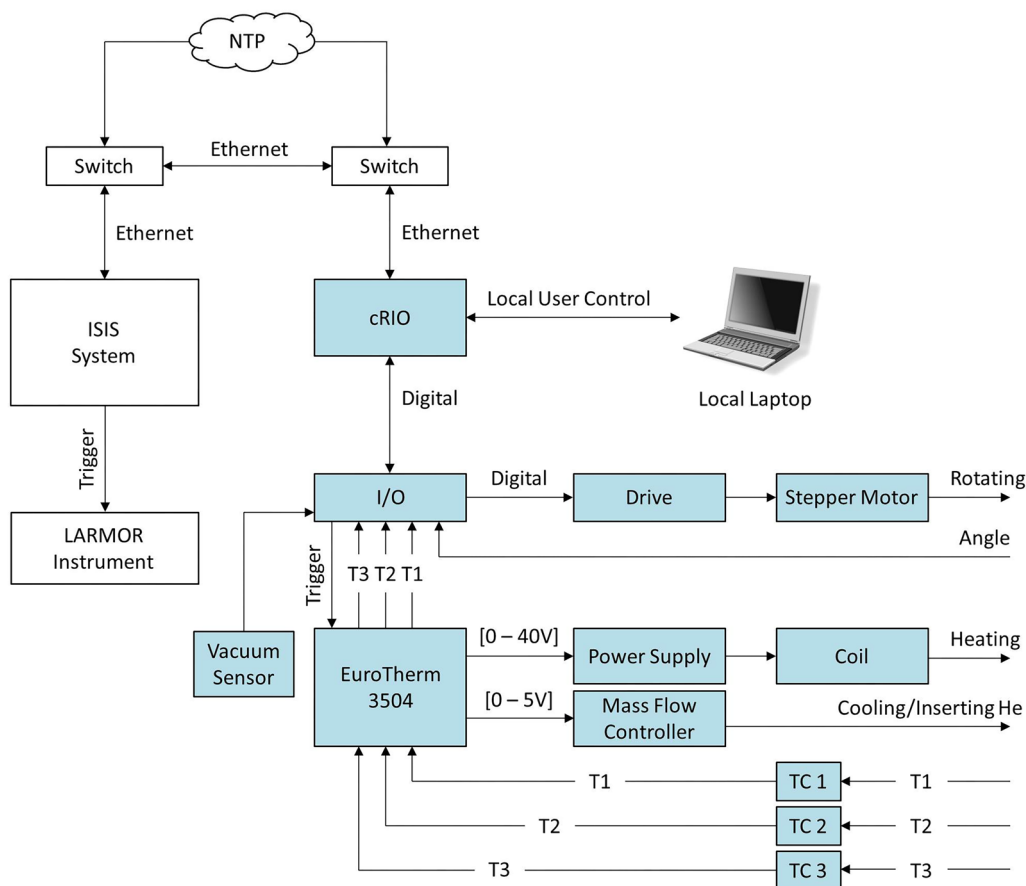
FIG. 4. Schematic illustration of the general control system setup and the connection diagram between all equipment needed to successfully perform the *in situ* SANS–ND measurements as well as the connection between this equipment and the ISIS control system.

V. *IN SITU* SIMULTANEOUS SANS–ND EXPERIMENTS

The first *in situ* SANS measurements in combination with ND measurements during the application of a specific thermal treatment with the designed furnace are carried out in the Larmor instrument at ISIS Neutron and Muon Source, at Rutherford Appleton Laboratory (UK). The final experimental setup is shown in Fig. 5. The size of the incident neutron beam is 8×8 mm^2 in order to measure a significant specimen volume and obtain good statistics in the resulting measurements. The specimen rotation is continuous during the application of the thermal treatments with a maximum rotation angle range of +18° (counter-clockwise direction).

A. Thermal treatments

Isothermal holding measurements at high temperatures are successfully applied in micro-alloyed steel specimens with distinct chemical compositions. Figure 6(a) shows an example of a thermal treatment applied by means of the developed furnace on a steel specimen with composition 0.071C–1.84Mn–0.29V (wt. %). This thermal treatment consists of continuous heating until full austenitization at a temperature (in this case, 1050 °C) at which all precipitates

are completely dissolved. After austenitization for several minutes, a rapid cooling process is applied by using helium gas for a short time followed by isothermal holding at 650 °C in vacuum (of the order of 10^{-4} mbar) for a certain period of time.
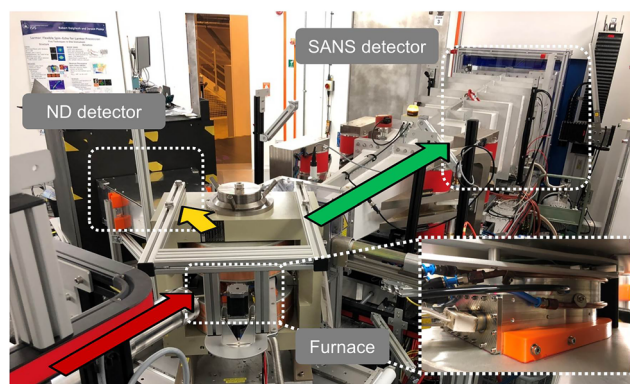

FIG. 5. Real experimental setup installed in Larmor instrument at ISIS Neutron and Muon Source, at Rutherford Appleton Laboratory (UK).
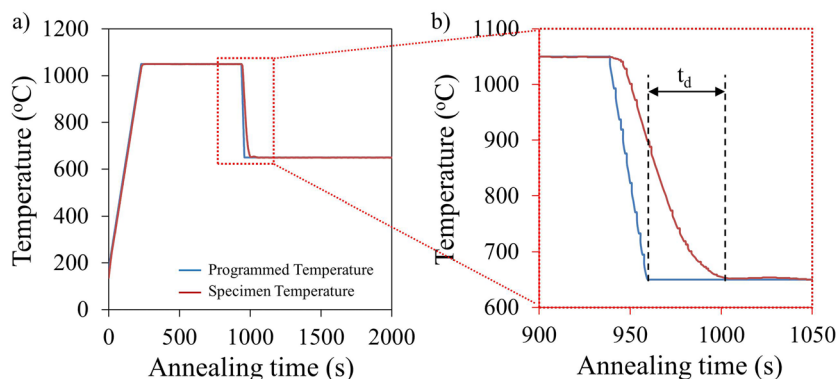
FIG. 6. Example of thermal treatment performed with the developed furnace during *in situ* and simultaneous SANS–ND measurements. A comparison between the programmed thermal profile and the specimen temperature recorded by a thermocouple is shown.

The response of the furnace is smooth in all stages of the programmed thermal profile due to the previous optimization of the PID values of the furnace control system. Only a small delay (t_d) is detected during the cooling stage, as observed in the enlarged image presented in Fig. 6(b). No large undercooling is detected during rapid cooling from austenitization to the isothermal temperature, avoiding the possible formation of precipitates before the isothermal holding.

B. Neutron diffraction

Figure 7 shows a comparison between the diffraction patterns of the empty furnace and the steel specimen after the background is subtracted, at a random time during the application of the isothermal holding at 650 °C. Both diffraction patterns are obtained through a neutron diffraction detector especially developed for these measurements. The diffraction pattern obtained from the empty furnace is recorded at room temperature. This pattern is considered to be the background signal and is subtracted from the diffraction signals obtained from the steel specimen. As observed in Fig. 7, several α-ferrite and γ-austenite diffraction peaks are observed during the austenite-to-ferrite phase transformation occurring in the steel specimen. After background subtraction, the evolution of the volume fractions of both phases as a function of holding time is calculated from the integrated intensity of these diffraction peaks. In this case, the intensity ratio between diffr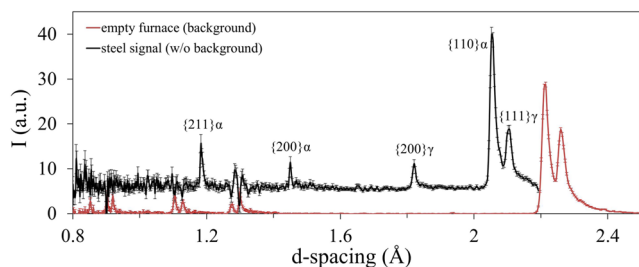action peaks of each phase remains constant as a function of time, indicating that the texture of the material remains unaltered during phase transformations.

Figure 8 shows the evolution of the {110}, {200}, and {211} α-ferrite diffraction peaks and the {111}, {200}, and {220} γ-austenite diffraction peaks obtained from a series of neutron diffraction measurements during the application of one-hour isothermal holding at 650 °C on the micro-alloyed steel specimen. The evolution of these diffraction peaks with time reveals the isothermal transformation of austenite into ferrite during holding. The austenite-to-ferrite transformation kinetics can be quantitatively analyzed from this series of neutron diffraction patterns.

C. Small angle neutron scattering

An example of a SANS pattern measured at a random time during the one-hour isothermal holding performed at 650 °C on a micro-alloyed steel specimen is shown in Fig. 9. The pattern includes the nuclear and magnetic contributions of the steel specimen. Sectors of 30° parallel and perpendicular to the applied magnetic field (*B*) are used to separate the nuclear and magnetic contributions

FIG. 7. Comparison between diffraction signals of the empty furnace and the steel specimen (after background subtraction) from neutron diffraction measurement at a random time during the isothermal holding at 650 °C. For a better distinction, the diffraction signal of the steel specimen is translated vertically with respect to that of the empty furnace.
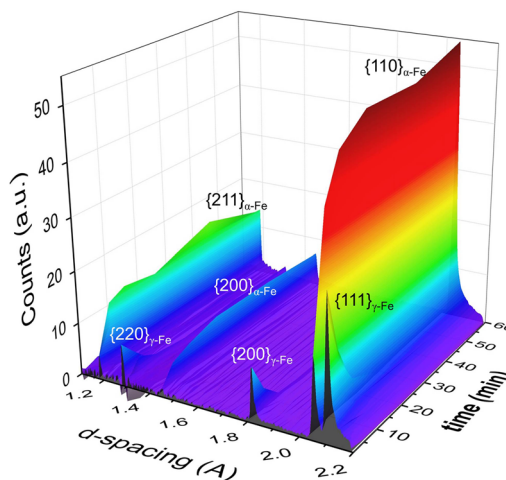

FIG. 8. Evolution of the diffraction peaks of α-ferrite and γ-austenite with time during one hour isothermal holding on a steel specimen, obtained from a series of neutron diffraction measurements.
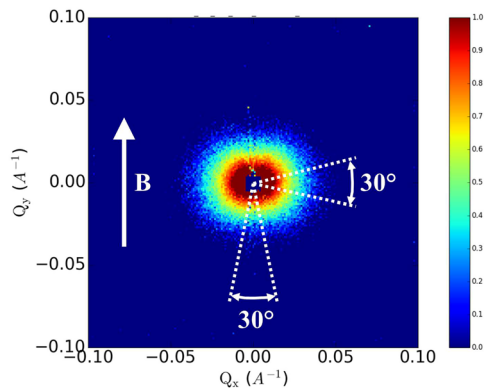
FIG. 9. Data obtained from a SANS measurement at a random time during the isothermal holding. The measurement includes the nuclear and magnetic contributions of the steel sample.

to the scattering. From these intensities, the precipitation kinetics, i.e., nucleation, growth, coarsening, and chemical composition of precipitates, is quantified following the procedure described in a previous study done by the authors of this article.[10]

Figure 10(a) shows an example of the *in situ* nuclear SANS intensity as a function of wave-vector transfer Q measured at specific times during the isothermal holding at 650 °C of the micro-alloyed steel specimen. As a comparison, Fig. 10(b) shows the corresponding *ex situ* nuclear SANS intensities measured at room temperature after the application of different holding times in the same type of steel specimens.[10] The intensity curves plotted in both figures are the result of the scattering originated only from the steel. This means that, in the case of the *in situ* measurements, the SANS intensity is corrected using the high-temperature SANS signal. The intensity curves of the *in situ* and *ex situ* SANS are measured at the same temperature–time conditions. For short measuring times (5 min–10 min curve), larger error bars are observed in the *in situ* SANS indicating a limitation to obtain good statistics for short isothermal treatments. This limitation can be avoided in the *ex situ* measurements where, in this case, a measuring time of 35 min is used to obtain good statistics since the measurement is performed after the application of the thermal treatment and all phase transformations and their related phenomena have already taken place.

On the other hand, the background subtraction is less challenging in the *in situ* measurements than in the *ex situ* ones. For the *in situ* SANS measurements, the background is considered as an intensity curve that includes no precipitate signal. This curve corresponds to the scattering signal of the fully austenitic microstructure obtained at high temperature, where precipitates are totally dissolved. This intensity curve is used as a reference and subtracted from the intensity curves obtained at distinct times during the isothermal holding in order to obtain the pure precipitate signal. For the *ex situ* SANS measurements, it is not possible to obtain a microstructure without dislocations to be used as a background reference. In this case, the intensity curve of the steel specimen directly quenched from the austenitization temperature to room temperature, whose microstructure consists of martensite with a high density of dislocations, should be considered as a (non-ideal)
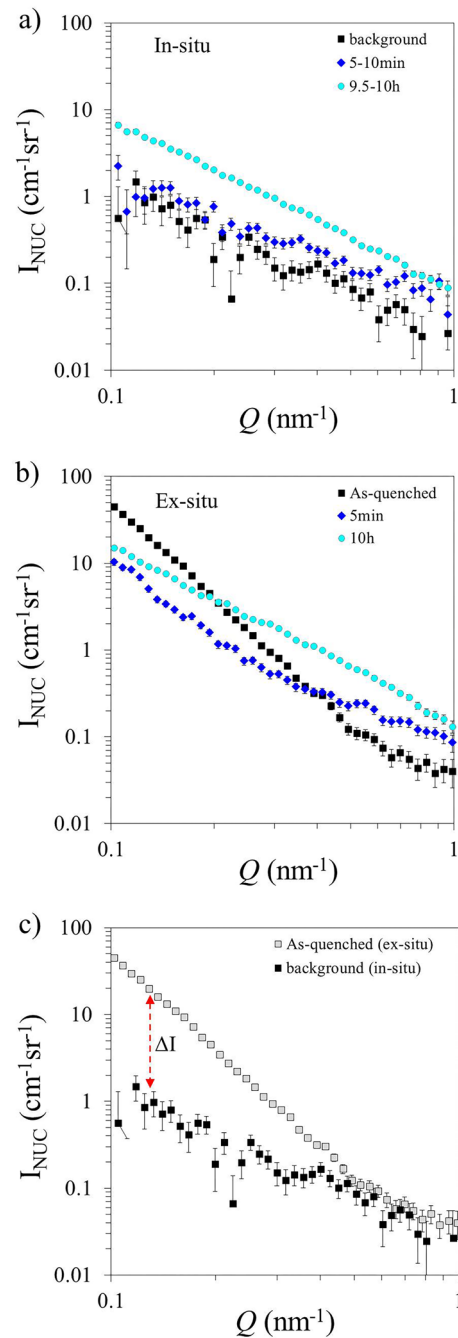

FIG. 10. Nuclear SANS intensity obtained from (a) *in situ* and (b) *ex situ* measurements during or after the application of isothermal holding at 650 °C in a micro-alloyed steel. (c) Comparison of possible background signals to be considered for later precipitation analysis derived from *in situ* and *ex situ* SANS measurements.

background signal. However, as shown in Fig. 10(b), this curve exhibits a higher intensity in the low-Q range than those curves obtained even after 10 h of holding time when the phase transformations and precipitation have already occurred.

The different background signal obtained in *in situ* and *ex situ* SANS measurements is a consequence of the different microstructure obtained in both steel specimens. Figure 10(c) shows a comparison of both background signals. The intensity difference (ΔI) at a lower-Q range between both specimens is related to the contribution to the SANS signal of the high dislocation density and iron carbides contained in the fully martensitic microstructure of the as-quenched specimen. Consequently, isolating the precipitate signal corresponding to the growth and coarsening of precipitates during the isothermal holding has proved to be more challenging in the case of *ex situ* SANS measurements since a more complicated procedure (including calculations of the background for different Q ranges) has to be followed. The discussion strongly supports performing *in situ* SANS measurements to study quantitatively the precipitation phenomenon and its kinetics in steels with higher accuracy.

VI. CONCLUSIONS

A furnace is designed and developed to perform *in situ* and simultaneous small-angle neutron scattering and neutron-diffraction measurements in micro-alloyed steels containing nano-precipitates. The furnace fulfills all the requirements needed to successfully carry out thermal treatments involving fast heating and cooling as well as high operation temperatures (up to 1200 °C), for a long period of time with an accurate control of the specimen temperature in a protective atmosphere and in a magnetic field. The development of this furnace allows the *in situ* study of interphase precipitation in steels by relating the nucleation, growth, and coarsening of precipitates to the kinetics of phase transformations occurring during the application of thermal treatments. This achievement not only opens new ways of research of the precipitation phenomenon in steels but also may stimulate developments of other furnaces for advanced research studies.

DATA AVAILABILITY

The data that support the findings of this study are openly available at https://doi.org/10.4121/13072076.

REFERENCES

[1] H. Halfa, "Recent trends in producing ultrafine grained steels," J. Miner. Mater. Charact. Eng. **02**, 428–469 (2014).

[2] H. J. Kong and C. T. Liu, "A review on nano-scale precipitation in steels," Technologies **6**(1), 36 (2018).

[3] N. H. van Dijk, W. G. Bouwman, S. E. Offerman, M. T. Rekveldt, J. Sietsma, S. van der Zwaag, A. Bodin, and R. K. Heenan, "High temperature SANS experiments on Nb(C,N) and MnS precipitates in HSLA steel," Metall. Mater. Trans. A **33**, 1883–1891 (2002).

[4] K. Osamura, H. Okuda, K. Asano, M. Furusaka, K. Kishida, F. Kurosawa, and R. Uemori, "SANS study of phase decomposition in Fe-Cu alloy with Ni and Mn addition," ISIJ Int. **34**, 346–354 (1994).

[5] E. G. Dere, H. Sharma, R. M. Huizenga, G. Portale, W. Bras, V. Bliznuk, J. Sietsma, and S. E. Offerman, "Formation of (Fe,Cr) carbides and dislocation structures in low-chromium steel studied in situ using synchrotron radiation," J. Appl. Cryst. **46**, 181–192 (2013).

[6] T. H. Simm, L. Sun, D. R. Galvin, E. P. Gilbert, D. Alba Venero, Y. Li, T. L. Martin, P. A. J. Bagot, M. P. Moody, P. Hill, H. K. D. H. Bhadeshia, S. Birosca, M. J. Rawson, and K. M. Perkins, "A SANS and APT study of precipitate evolution and strengthening in a maraging steel," Mater. Sci. Eng.: A **702**, 414–424 (2017).

[7] R. Okamoto, A. Borgenstam, and J. Ågren, "Interphase precipitation in niobium-microalloyed steels," Acta Mater. **58**, 4783–4790 (2010).

[8] Y. Oba, S. Koppoju, M. Ohnuma, T. Murakami, H. Hatano, K. Sasakawa, A. Kitahara, and J.-i. Suzuki, "Quantitative analysis of precipitate in vanadium-microalloyed medium carbon steels using small-angle X-ray and neutron scattering methods," ISIJ Int. **51**, 1852–1858 (2011).

[9] Y. Q. Wang, S. J. Clark, V. Janik, R. K. Heenan, D. A. Venero, K. Yan, D. G. McCartney, S. Sridhar, and P. D. Lee, "Investigating nano-precipitation in a V-containing HSLA steel using small angle neutron scattering," Acta Mater. **145**, 84–96 (2018).

[10] C. Ioannidou, Z. Arechabaleta, A. Navarro-López, A. Rijkenberg, R. M. Dalgliesh, S. Kölling, V. Bliznuk, C. Pappas, J. Sietsma, A. A. van Well, and S. E. Offerman, "Interaction of precipitation with austenite-to-ferrite phase transformation in vanadium micro-alloyed steels," Acta Mater. **181**, 10–24 (2019).

[11] F. Perrard, A. Deschamps, F. Bley, P. Donnadieu, and P. Maugis, "A small-angle neutron scattering study of fine-scale NbC precipitation kinetics in the α-Fe–Nb–C system," J. Appl. Cryst. **39**, 473–482 (2006).

[12] B. S. Seong, E. Shin, S.-H. Choi, Y. Choi, Y. S. Han, K. H. Lee, and Y. Tomota, "Quantitative analysis of fine nano-sized precipitates in low-carbon steels by small angle neutron scattering," Appl. Phys. A **99**, 613–620 (2010).

[13] S. Dhara, R. K. W. Marceau, K. Wood, T. Dorin, I. B. Timokhina, and P. D. Hodgson, "Precipitation and clustering in a Ti-Mo steel investigated using atom probe tomography and small-angle neutron scattering," Mater. Sci. Eng.: A **718**, 74–86 (2018).

[14] M. G. Bowman, D. E. Hull, W. G. Witteman, G. P. Arnold, and A. L. Bowman, "High temperature neutron diffraction furnace," Rev. Sci. Instrum. **37**, 1543–1544 (1966).

[15] F. P. Bailey and C. E. G. Bennett, "A simple furnace for neutron diffraction studies," J. Appl. Cryst. **12**, 403–404 (1979).

[16] S. Katano, H. Motohashi, and M. Iizumi, "Furnace for rapid change of temperature for neutron diffraction," Rev. Sci. Instrum. **57**, 1409–1412 (1986).

[17] T. Flottmann, W. Petry, R. Serve, and G. Vogl, "A combined furnace for crystal growth and neutron scattering," Nucl. Instrum. Methods Phys. Res., Sect. A **260**, 165–170 (1987).

[18] L. Margulies, M. J. Kramer, R. W. McCallum, S. Kycia, D. R. Haeffner, J. C. Lang, and A. I. Goldman, "New high temperature furnace for structure refinement by powder diffraction in controlled atmosphere using synchrotron radiation," Rev. Sci. Instrum. **70**, 3554–3561 (1999).

[19] P. Staron, E. Eidenberger, M. Schober, M. Sharp, H. Leitner, A. Schreyer, and H. Clemens, "*In situ* small-angle neutron scattering study of the early stages of precipitation in Fe-25 at.% Co-9 at.% Mo and Fe-1 at.% Cu at 500 °C," J. Phys.: Conf. Ser. **247**, 012038 (2010).

[20] H. M. Reiche, S. C. Vogel, P. Mosbrucker, E. J. Larson, and M. R. Daymond, "A furnace with rotating load frame for *in situ* high temperature deformation and creep experiments in a neutron diffraction beam line," Rev. Sci. Instrum. **83**, 053901 (2012).

[21] P. A. Shade, B. Blank, J. C. Schuren, T. J. Turner, P. Kenesei, K. Goetze, R. M. Suter, J. V. Bernier, S. F. Li, J. Lind, U. Lienert, and J. Almer, "A rotational and axial motion system load frame insert for in-situ high-energy X-ray studies," Rev. Sci. Instrum. **86**, 093902 (2015).

[22] D. C. Pagan, J. V. Bernier, D. Dale, J. Y. P. Ko, T. J. Turner, B. Blank, and P. A. Shade, "Measuring Ti-7Al slip system strengths at elevated temperature using high-energy X-ray diffraction," Scr. Mater. **142**, 96–100 (2018).

[23] H. Sharma, A. C. Wattjes, M. Amirthalingam, T. Zuidwijk, N. Geerlofs, and S. E. Offerman, "Multipurpose furnace for *in situ* studies of polycrystalline materials using synchrotron radiation," Rev. Sci. Instrum. **80**, 123301 (2009).

[24] C. Ioannidou, A. Navarro-López, A. Rijkenberg, R. M. Dalgliesh, S. Kölling, C. Pappas, J. Sietsma, A. A. van Well, and S. E. Offerman, "Evolution of the precipitate chemical composition during annealing of vanadium micro-alloyed steels by in-situ SANS," Acta Mater. **201**, 217 (2020).

[25] J. Fenske, M. Rouijaa, J. Šaroun, R. Kampmann, P. Staron, G. Nowak, J. Pilch, P. Beran, P. Šittner, P. Strunz, H.-G. Brokmeier, V. Ryukhtin, L. Kaděřávek, M. Strobl, M. Müller, P. Lukáš, and A. Schreyer, "BEER – The beamline for

European materials engineering research at the ESS," J. Phys.: Conf. Ser. **746**, 012009 (2016).

[26] See http://www.gmw.com/electromagnets/dipole/3473/3473_Specs for a detailed description of specifications of the GMW-3473 dipole electromagnet.

[27] T. Gnäupel-Herold and A. Creuziger, "Diffraction study of the retained austenite content in TRIP steels," Mater. Sci. Eng.: A **528**, 3594–3600 (2011).

[28] F. A. Akeroyd, K. V. L. Baker, M. J. Clarke, J. R. Holt, G. D. Howells, D. P. Keymer, T. Löhnert, C. M. Moreton-Smith, D. E. Oram, A. Potter, I. H. Rey, T. A. Willemsen, and K. Woods, "IBEX - an EPICS based control system for the ISIS pulsed neutron and muon source," J. Phys.: Conf. Ser. **1021**, 012019 (2018).

[29] S. E. Offerman, E. van der Wal, A. A. van Well, A. Navarro-López, C. Ioannidou, and R. M. Dalgliesh, "*In-situ* and simultaneous SANS and ND to study the precipitation and phase transformation kinetics in V-containing nano-steels," STFC ISIS Neutron and Muon Source, 2019, https://doi.org/10.5286/ISIS.E.RB1869024.